

Nicotine as a Catalyst for Chlorination Promoted by Hypochlorous Acid: Experimental and Theoretical Studies

Valdecir F. Ximenes,[✉]*^a Nathalia M. Pavan,^a Aginaldo R. de Souza,^a
Gabriel A. Barros^b and Nelson H. Morgon[✉]*^b

^aDepartamento de Química, Faculdade de Ciência,
Universidade Estadual Paulista (UNESP), 17033-360 Bauru-SP, Brazil

^bDepartamento de Físico-Química, Instituto de Química,
Universidade Estadual de Campinas (UNICAMP), 13083-861 Campinas-SP, Brazil

There is robust evidence of the hypochlorous acid (HClO)-mediated damage in biomolecules, and nicotine boosts the chlorination potency of HClO. We present experimental and theoretical evidence of the mechanism by which nicotine catalyzes the chlorination of pyranine. The rate constants for chlorination of pyranine by HClO were measured in the presence ($5.3 \times 10^5 \text{ mol}^{-1} \text{ L s}^{-1}$) and absence of nicotine ($4.2 \times 10^3 \text{ mol}^{-1} \text{ L s}^{-1}$), revealing the catalytic effect of the alkaloid. Density functional theory (DFT) calculations, based on B3LYP-GD3(BJ)/6-311++G(3df,2p)/SMD(Water)//B3LYP-GD3(BJ)/6-311++G(2d,p)/SMD(Water) level of theory, were performed and showed a decreased activation energy for chlorine transfer and hydrogen abstraction when nicotine chloramine intermediated the reaction. The atomic polar tensor (APT) charges on the chlorine atom of HClO (+0.084) were lower than the chlorine of nicotine chloramine (+0.149), revealing the higher electrophilic character of nicotine chloramine. In conclusion, the increased electrophilic nature of HClO provoked by nicotine explains its catalytic effect.

Keywords: hypochlorous acid, nicotine, chlorination of biomolecules, DFT calculations

Introduction

Nicotine is a naturally occurring toxic alkaloid, the primary addictive component of tobacco smoke, and is directly involved in the harmful effect of the smoking habit.¹⁻³ The role of nicotine in atherosclerosis progression,⁴ vascular function impairment,⁵ induction of cell-cycle progression, angiogenesis, metastasis of lung cancers, and detrimental effects on lung function are just a few reports of a multitude of harmful effects of nicotine.⁶ Reactive oxygen species (ROS) play an important role in the detrimental effect of nicotine. For instance, the nicotine-induced autophagy and neurological changes in human neuroglia cells,⁷ the augmented mitochondrial ROS level in cardiomyocyte hypertrophy, fibrosis, and inflammation in rat hearts.⁸

Among the ROS, hypochlorous acid (HClO) deserves special attention in this work. HClO is an endogenous chemical generated by myeloperoxidase (MPO)-catalyzed oxidation of chloride in activated neutrophils.⁹ From a

physiological point of view, it plays an essential role in the innate immune response as a microbicidal agent.¹⁰ However, it also has a pathological role, as there is considerable evidence of its involvement in proteins,¹¹ nucleic acids,¹² and lipids¹³ degradation.

In 1998, Prütz¹⁴ demonstrated that HClO-induced chlorination of salicylate, alkenes, and thymidine were sped up by adding catalytic amounts of trimethylamine and quinine. Following this work, several other publications reinforced tertiary amines' catalytic effect on HClO-mediated chlorination and oxidation of biomolecules. For instance, the degradation of nicotinamide adenine dinucleotide (NADH),¹⁵ and the reaction of nicotine with HClO leading to nicotine chloramine, which provoked dose-dependent damage to proliferating cell nuclear antigen (PCNA).¹⁶ Other examples are the use of nicotine and trimethylamine to promote the chlorination of free (2'-deoxy)nucleosides and nucleosides in ribonucleic acid (RNA),¹⁷ uracyl chlorination,¹⁸ and low-density lipoprotein oxidation.¹⁹ Due to the biological relevance of HClO, its reaction with antioxidants has been theoretically investigated. An interesting example is the reaction of HClO

*e-mail: valdecir.ximenes@unesp.br; nhmorgon@gmail.com

Editor handled this article: José Walkimar M. Carneiro

with the endogenous antioxidant carnosine. In this work, high-level *ab initio* calculations were performed to show that Cl^+ shift was the rate-determining step, with a barrier of $109.5 \text{ kJ mol}^{-1}$ relative to the reactant, in which carnosine is chlorinated in the imidazole ring.²⁰ Based on the relevance of the theme, this work presents a contribution to advance in the comprehension of the harmful effect of nicotine as a catalyst for HClO-based chlorination.

Experimental

Chemicals

Nicotine and pyranine (trisodium 8-hydroxypyrene-1,3,6-trisulfonate) were purchased from Sigma-Aldrich Chemical Co. (St. Louis, MO, USA). The concentration of the commercial sodium hypochlorite (12%) solution was determined spectrophotometrically after dilution in 0.01 mol L^{-1} NaOH at pH 12 (molar absorption coefficient at 292 nm ($\epsilon_{292\text{nm}}$) = $350 \text{ mol}^{-1} \text{ L cm}^{-1}$).²¹ The solution of HClO was prepared immediately before the assays to give an aqueous stock solution of 100 mmol L^{-1} .

Determination of rate constants

The fast-kinetic experiments were performed using a single-mixing stopped-flow system equipped with a high-intensity light-emitting diode (LED) source and cut-off filters (SX20/LED Stopped-Flow System, Applied Photophysics, Leatherhead, UK). The experiments were performed at room temperature using pseudo-first-order conditions. The HClO was used in excess ($20\text{--}80 \mu\text{mol L}^{-1}$) compared to a fixed concentration of pyranine ($1.0 \mu\text{mol L}^{-1}$) in 50 mmol L^{-1} phosphate buffer, pH 7.0. The time-dependent consumption of pyranine was monitored by its fluorescence bleaching using a 435-nm LED for excitation and a cut-off 515 nm filter for emission.

The overall bimolecular rate constants (k) were calculated as follows (equation 1):

$$\text{Reaction rate (fluorescence decay)} = k \times [\text{HClO}] \times [\text{pyranine}] \quad (1)$$

Assuming pseudo-first-order condition, $[\text{HClO}] \gg [\text{pyranine}]$, one have (equation 2):

$$\text{Reaction rate (fluorescence decay)} = k_{\text{obs}} \times [\text{pyranine}] \quad (2)$$

As $k_{\text{obs}} = k \times [\text{HClO}]$, k can be obtained from the slope of the linear fit of k_{obs} versus $[\text{HClO}]$.

Experimentally, k_{obs} were obtained by fitting the experimental data (fluorescence decay at increasing

concentration of HClO) to single exponential decay (equation 3).²²

$$F = F_0 \times e^{-k_{\text{obs}} \times t} \quad (3)$$

where, t : time, F : fluorescence at any time, F_0 : fluorescence at time zero.

Computational methods

Electronic and molecular structures were calculated using density functional theory (DFT) calculations on the ground state of all molecules. The full optimization structures of all molecular systems were obtained at B3LYP/6-311++G(2df,p) level of theory. The Synchronous Transit-guided Quasi-Newton methods (QST2 or QST3) were employed to look for transition states at the same level of theory. The stationary points (minima or transition states) were confirmed by calculating the harmonic vibrational frequencies. The connectivity of the transition states and local minima were confirmed via intrinsic reaction coordinate (IRC) calculations using the Hessian-based Predictor-Corrector (HPC) algorithm (see Supplementary Information (SI section) for additional details, Figures S1-S5).²³ These calculations were carried out to verify the nature of these transition states (TS) and demonstrate that they are connected to stationary species as minima. The single point energies were refined by B3LYP/6-311++G(2d,p) calculations. The solvent effects (water) were calculated with the Solvation Model Based on Density (SMD) model,²⁴ and the D3 version of Grimme's dispersion with Becke-Johnson damping was added to all calculations.^{25,26} This level of theory can be denoted as B3LYP-GD3(BJ)/6-311++G(3df,2p)/SMD(Water)//B3LYP-GD3(BJ)/6-311++G(2d,p)/SMD(Water). All calculations were performed using the Gaussian 16 program.²⁷

Results and Discussion

Several evidence of the catalytic effect of tertiary amines, including nicotine, in HClO-mediated reactions, have been reported.^{14,15,17-19} Here, pyranine was used as a fluorescent polyaromatic compound to study, experimentally and theoretically, the catalytic effect of nicotine. Pyranine has been used as a fluorescent probe to study redox processes of biological relevance. Notably, its reaction with HClO has been used to monitor the antioxidant activity of polyphenols via pyranine fluorescence bleaching.²⁸ Here, this feature was confirmed, as the consumption of pyranine by HClO caused the fluorescence loss without the formation of other detectable fluorescent products (Figure S6, SI section).

As pyranine has its excitation (435 nm) and emission (515 nm) far from the absorption of nicotine (250 nm) and HClO (292 nm), its consumption can be easily monitored without spectral interference. Figure 1a shows the bleaching of the pyranine fluorescence provoked by the addition of HClO. As it can be seen, while the chlorination of pyranine was completed in less than 1 s in the presence of nicotine, in its absence, the consumption took place in around 60 s. From these findings, the reaction kinetics was studied in pseudo-first-order condition (excess of HClO), and the bimolecular rate constants (k) were determined in the absence and presence of nicotine (see Experimental section for details, Figures 1b and 1c). As shown, in the presence of nicotine, k was $5.3 \times 10^5 \text{ mol}^{-1} \text{ L s}^{-1}$. In its absence, the value was $4.2 \times 10^3 \text{ mol}^{-1} \text{ L s}^{-1}$, revealing a two-order of magnitude increase and confirming the catalytic effect on chlorination of aromatic compounds.

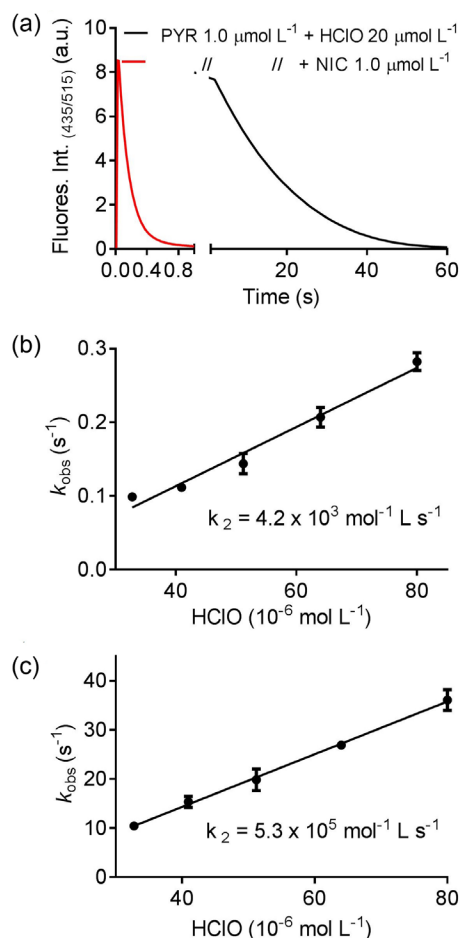


Figure 1. Determination of bimolecular rate constant for the reaction between pyranine and HClO and the effect of nicotine as a catalyst. (a) Representative example of fluorescence decay of pyranine due to its reaction with HClO in the absence and presence of nicotine. Pyranine $1.0 \mu\text{mol L}^{-1}$, HClO $20 \mu\text{mol L}^{-1}$, and nicotine $1.0 \mu\text{mol L}^{-1}$ in 50 mmol L^{-1} phosphate buffer, pH 7.0, 25°C . (b, c) Determination of bimolecular rate constant in the absence (b) and presence (c) of nicotine. The results are the mean of three experiments and standard deviation (error bars).

Once the catalytic effect of nicotine on the chlorination of aromatic compounds via HClO was proved, DFT calculations were carried out to elucidate the proposed mechanism. The calculations were performed assuming a mechanism based on the electrophilic attack of HClO or nicotine chloramine on the aromatic ring. It can be outlined as follows (Scheme 1).

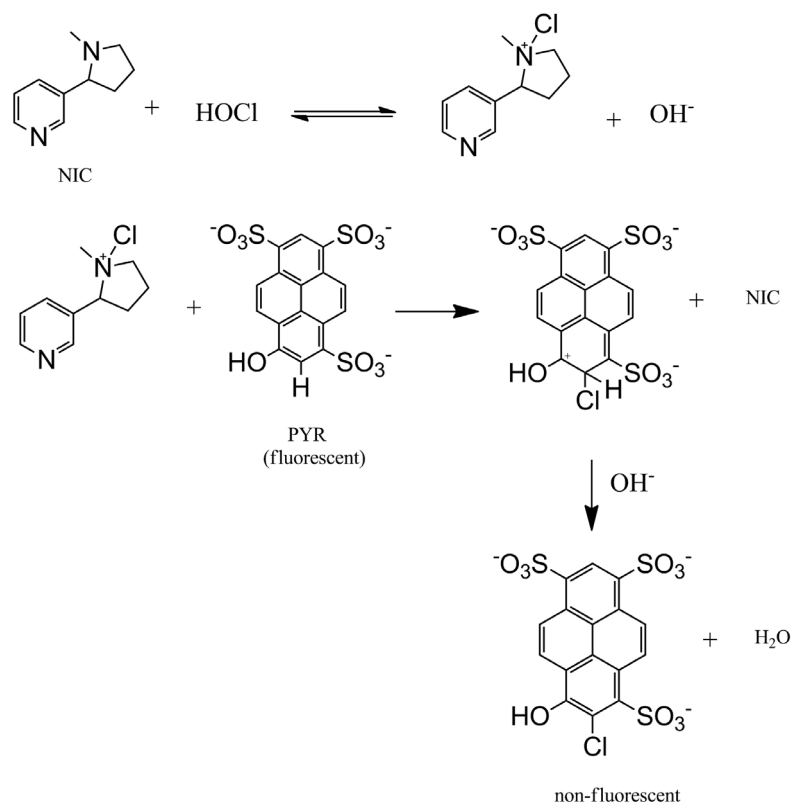
DFT study, mechanism 1: HClO as the electrophile

In the proposed theoretical mechanism, step 1 involves the formation of a van der Waals complex between HClO and pyranine. This process leads to a transition state (TS) where the chlorine atom is shared by the hydroxyl of HClO and the carbon atom (C1) at the pyranine ring (Scheme 2). The bond lengths that characterized the process HO---Cl---C(pyranine) were equal to 1.92 \AA and 2.42 \AA , respectively. This TS was characterized by the imaginary harmonic vibrational frequency (230.67 cm^{-1}) associated with the normal mode of vibration simultaneously shared by the two groups of atoms bound to chlorine (Figure S7, SI section). In step 2, the removal of the hydrogen atom attached to C1 took place. For that, the released HO^- , from the medium, bound to the C2 leading to a second intermediate. In the next step, an intramolecular hydrogen atom transfer and the subsequent water loss took place.

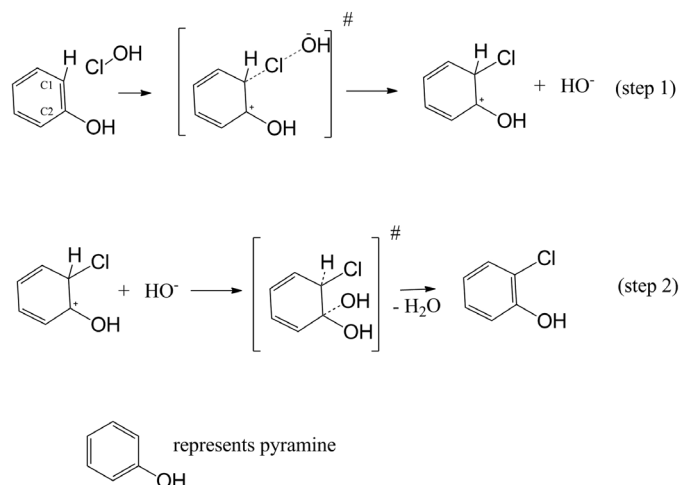
DFT study, mechanism 2: nicotine chloramine as the electrophile

The preliminary step in the theoretical proposed mechanism is the interaction between nicotine and HClO to generate nicotine chloramine. The approximation of HClO formed a van der Waals complex and was followed by a TS where the chlorine atom was shared by the nitrogen atom (pyrrolidine ring) and the hydroxyl group of HClO. The geometric parameters (atomic distances) that characterized the TS: HO---Cl---N(nicotine) were equal to 3.22 \AA and 1.79 \AA , respectively. The normal vibration mode showed an imaginary frequency of 236.57 cm^{-1} (Scheme 3, step 1, Figure S8, SI section).

In the next step of the mechanism, the nicotine chloramine attacks the pyranine ring. This step involved the formation of a van der Waals complex followed by the transfer of the chlorine atom via TS, which presented an imaginary frequency of 241.87 cm^{-1} and was characterized by the bond distances N(nicotine)---Cl---C1(pyranine) equal to 2.40 \AA and 1.94 \AA , respectively (Scheme 3, step 2, Figure S9, SI section). In the sequence, the hydroxyl anion from the medium forms a chemical bond to the C2 atom, and a water molecule is released. The TS, for this process,



Scheme 1. Mechanistic proposal for the catalytic effect of nicotine (NIC) on the chlorination of pyranine (PYR).

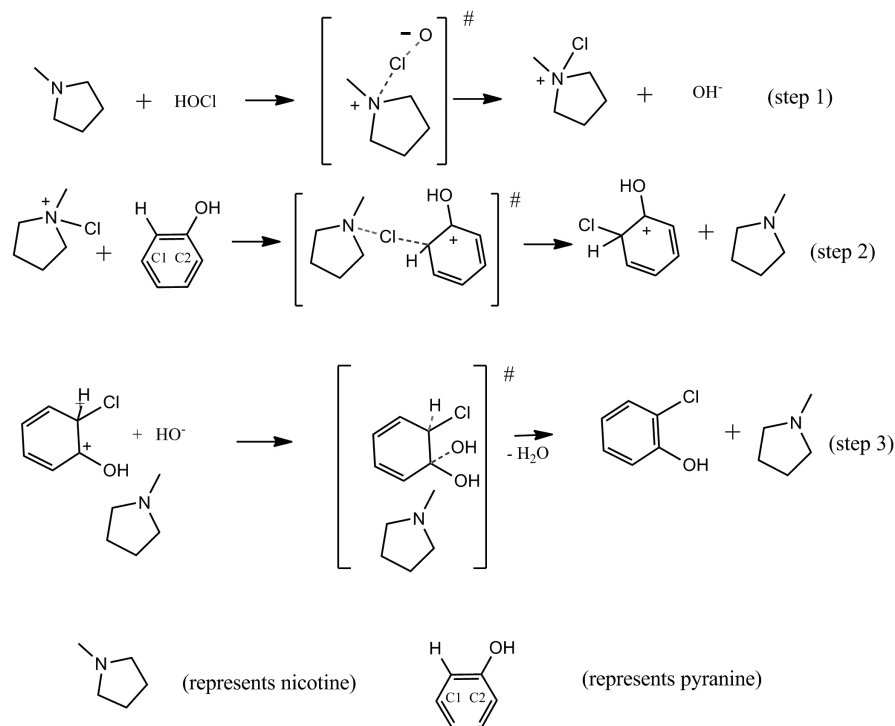


Scheme 2. DFT-based proposed mechanism for the chlorination of pyranine in the absence of nicotine.

was characterized by the bond distances: C---H---O equal to 1.14 Å and 1.71 Å, respectively, and the imaginary frequency 619.75 cm⁻¹ (Scheme 3, step 3, Figure S10, SI section).

The reaction coordinates and Gibbs energies for all steps are depicted in Figure 2. The activation energies of the reactions, obtained through DFT simulations, are shown in Table 1. The electronic energies and cartesian coordinates are available in the SI section (Tables S1 to S18). The molecular electrostatic potential (MEP) maps are often used for the qualitative interpretation of electrophilic and nucleophilic

reactions. They were obtained using the atomic polar tensor charges, calculated at B3LYP-GD3(BJ)/6-311++G(3df,2p)/SMD(Water) level of theory. In our study, the atomic polar tensor charges on the Cl atom were +0.084 (HClO) and +0.149 (Nicotine-Cl), revealing the higher electrophilic character of the last (Figure S11, SI section). These findings showed that the increased electrophilicity superimposed the negative impact of approximation of the bulky Nicotine-Cl group toward the aromatic ring. The same result was obtained for the chlorination of salicylate using quinine as the catalyst.



Scheme 3. DFT-based proposed mechanism for the chlorination of pyranine in the presence of nicotine.

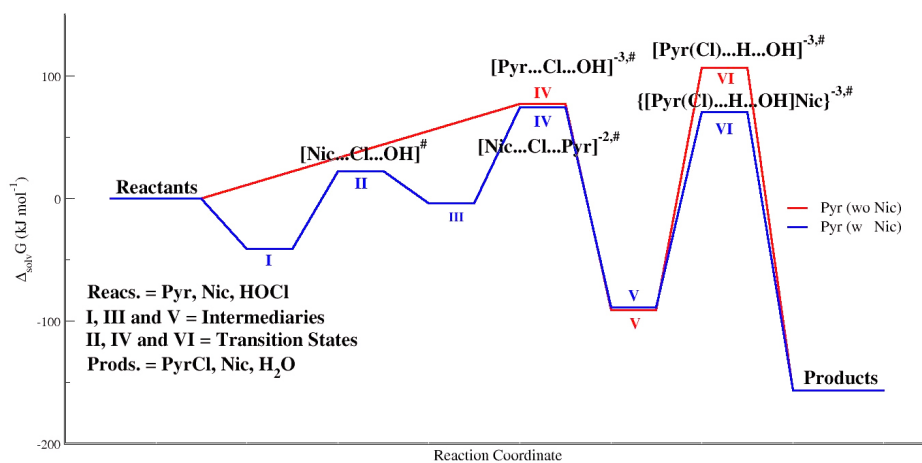


Figure 2. Reaction coordinates for the chlorination of pyranine in the presence and absence of nicotine.

Table 1. Density functional theory (DFT)-simulated activation energies in the presence and absence of nicotine

System	EA / (kJ mol ⁻¹)	
	Absence of nicotine	Presence of nicotine
[Pyr...Cl...OH] ^{-3,#} (k1)	86.52160	–
[Pyr(Cl)...H...OH] ^{-3,#} (k2)	123.92780	–
[Nic...Cl...OH] [#] (k3)	–	24.559180
[Nic...Cl...Pyr] ^{-2,#} (k4)	–	75.994595
[Pyr(Cl)...H...OH](Nic) ^{-3,#} (k5)	–	90.463923

Pyr: pyranine; Nic: nicotine; EA: activation energies.

It is worth noting that azabicyclo moiety of quinine is still more sterically crowded than Nicotine-Cl.¹⁴

Conclusions

In conclusion, by decreasing the activation energies of chlorine transfer and hydrogen abstraction, nicotine catalyzed the chlorination of pyranine. The atomic polar tensor charges revealed the higher electrophilic character of the chlorine atom on the nicotine intermediate, reinforcing the role of the alkaloid as a catalyst. These theoretical findings could explain the reported effects of nicotine as a catalyst for the chlorination of biomolecules.

Supplementary Information

Supplementary data are available free of charge at <http://jbcbs.sbq.org.br> as PDF file.

Acknowledgments

This work has been financed by National Council for Scientific and Technological Development (CNPq, grant: 303485/2019-1 and 303581/2018-2), Coordination for the Improvement of Higher Education Personnel (CAPES, Finance Code 001, 88887.612536/2021-00 and 88887.194785/2018-00), National Institute of Science and Technology - INCT BioNat, grant: 465637/2014-0, State of Sao Paulo Research Foundation (FAPESP, grant: 2019/18445-5 and 2019/12294-5).

References

- Schaal, C.; Chellappan, S. P.; *Mol. Cancer Res.* **2014**, *12*, 14. [Crossref]
- Jaimes, E. A.; Zhou, M.-S.; Siddiqui, M.; Rezonzew, G.; Tian, R.; Seshan, S. V.; Muwonge, A. N.; Wong, N. J.; Azelglu, E. U.; Fornoni, A.; Merscher, S.; Raij, L.; *Am. J. Physiol. Renal* **2021**, *320*, 442. [Crossref]
- Gould, G. S.; Havard, A.; Lim, L. L.; Group, T. P. S. P. E.; Kumar, R.; *Int. J. Environ. Res. Public Health* **2020**, *17*, 2034. [Crossref]
- Fu, X.; Zong, T.; Yang, P.; Li, L.; Wang, S.; Wang, Z.; Li, M.; Li, X.; Zou, Y.; Zhang, Y.; Aung, L. H. H.; Yang, Y.; Yu, T.; *Food Chem. Toxicol.* **2021**, *151*, 112154. [Crossref]
- Babic, M.; Schuchardt, M.; Tölle, M.; van der Giet, M.; *Eur. J. Clin. Invest.* **2019**, *49*, e13077. [Crossref]
- Nguyen, H. M. H.; Torres, J. A.; Agrawal, S.; Agrawal, A.; *Mediators Inflammation* **2020**, *2020*, ID 6705428. [Crossref]
- Feng, Y.; Xu, F.; Wang, S. M.; Wu, S. X.; Zhang, X. H.; Gao, Y. X.; Li, Y. L.; Zhong, D. B.; Yin, J. Z.; Feng, Y. M.; *Int. J. Neurosci.* **2019**, *130*, 391. [Crossref]
- Ramalingam, A.; Budin, S. B.; Fauzi, N. M.; Ritchie, R. H.; Zainalabidin, S.; *Sci. Rep.* **2021**, *11*, 13845. [Crossref]
- Panasenko, O. M.; Gorudko, I. V.; Sokolov, A. V.; *Biochemistry (Moscow)* **2013**, *78*, 1466. [Crossref]
- Winterbourn, C. C.; Kettle, A. J.; Hampton, M. B.; *Annu. Rev. Biochem.* **2016**, *85*, 765. [Crossref]
- Hawkins, C. L.; *Essays Biochem.* **2020**, *64*, 75. [Crossref]
- Macer-Wright, J. L.; Sileikaite, I.; Rayner, B. S.; Hawkins, C. L.; *Chem. Res. Toxicol.* **2020**, *33*, 402. [Crossref]
- Ford, D. A.; *Clin. Lipidol.* **2010**, *5*, 835. [Crossref]
- Prütz, W. A.; *Arch. Biochem. Biophys.* **1998**, *357*, 265. [Crossref]
- Prütz, W. A.; Kissner, R.; Koppenol, W. H.; *Arch. Biochem. Biophys.* **2001**, *393*, 297. [Crossref]
- Salama, S. A.; Arab, H. H.; Omar, H. A.; Maghrabi, I. A.; Snapka, R. M.; *Inflammation* **2014**, *37*, 785. [Crossref]
- Masuda, M.; Suzuki, T.; Friesen, M. D.; Ravanat, J. L.; Cadet, J.; Pignatelli, B.; Nishino, H.; Ohshima, H.; *J. Biol. Chem.* **2001**, *276*, 40486. [Crossref]
- Takeshita, J.; Byun, J.; Nhan, T. Q.; Pritchard, D. K.; Pennathur, S.; Schwartz, S. M.; Chait, A.; Heinecke, J. W.; *J. Biol. Chem.* **2006**, *281*, 3096. [Crossref]
- Oliveira, O. M. M. F.; Brunetti, I. L.; Khalil, N. M.; *An. Acad. Bras. Cienc.* **2015**, *87*, 183. [Crossref]
- Karton, A.; O'Reilly, R. J.; Pattison, D. I.; Davies, M. J.; Radom, L.; *J. Am. Chem. Soc.* **2012**, *134*, 19240. [Crossref]
- Ximenes, V. F.; Morgon, N. H.; de Souza, A. R.; *J. Inorg. Biochem.* **2015**, *146*, 61. [Crossref]
- Bertoza, L. C.; Morgon, N. H.; de Souza, A. R.; Ximenes, V. F.; *Biomolecules* **2016**, *6*, 23. [Crossref]
- Hratchian, H. P.; Schlegel, H. B.; *J. Chem. Phys.* **2004**, *120*, 9918. [Crossref]
- Marenich, A. V.; Cramer, C. J.; Truhlar, D. G.; *J. Phys. Chem. B* **2009**, *113*, 6378. [Crossref]
- Grimme, S.; Ehrlich, S.; Goerigk, L.; *J. Comput. Chem.* **2011**, *32*, 1456. [Crossref]
- Smith, D. G. A.; Burns, L. A.; Patkowski, K.; Sherrill, C. D.; *J. Phys. Chem. Lett.* **2016**, *7*, 2197. [Crossref]
- Frisch, M. J.; Trucks, G. W.; Schlegel, H. B.; Scuseria, G. E.; Robb, M. A.; Cheeseman, J. R.; Scalmani, G.; Barone, V.; Petersson, G. A.; Nakatsuji, H.; Li, X.; Caricato, M.; Marenich, A. V.; Bloino, J.; Janesko, B. G.; Gomperts, R.; Mennucci, B.; Hratchian, H. P.; Ortiz, J. V.; Izmaylov, A. F.; Sonnenberg, J. L.; Williams, D. J.; Ding, F.; Lipparini, F.; Egidi, F.; Goings, J.; Peng, B.; Petrone, A.; Henderson, T.; Ranasinghe, D.; Zakrzewski, V. G.; Gao, J.; Rega, N.; Zheng, G.; Liang, W.; Hada, M.; Ehara, M.; Toyota, K.; Fukuda, R.; Hasegawa, J.; Ishida, M.; Nakajima, T.; Honda, Y.; Kitao, O.; Nakai, H.; Vreven, T.; Throssell, K.; Montgomery Jr., J. A.; Peralta, J. E.; Ogliaro, F.; Bearpark, M. J.; Heyd, J. J.; Brothers, E. N.; Kudin, K. N.; Staroverov, V. N.; Keith, T. A.; Kobayashi, R.; Normand, J.; Raghavachari, K.; Rendell, A. P.; Burant, J. C.; Iyengar, S. S.; Tomasi, J.; Cossi, M.; Millam, J. M.; Klene, M.; Adamo, C.; Cammi, R.; Ochterski, J. W.; Martin, R. L.; Morokuma, K.; Farkas, O.; Foresman, J. B.; Fox, D. J.; *Gaussian 16, Revision C.01*; Gaussian, Inc., Wallingford CT, 2016. [Link] accessed in June 2022
- Pérez-Cruz, F.; Cortés, C.; Atala, E.; Bohle, P.; Valenzuela, F.; Olea-Azar, C.; Speisky, H.; Aspée, A.; Lissi, E.; López-Alarcón, C.; Bridi, R.; *Molecules* **2013**, *18*, 1638. [Crossref]

Submitted: January 18, 2022

Published online: June 27, 2022

